Scattering of guided waves at delaminations in composite plates

Bibi I.S. Murat [a], Pouyan Khalili [b], and Paul Fromme [a]

[a] Department of Mechanical Engineering, University College London, WC1E 7JE, UK

[b] Department of Mechanical Engineering, Imperial College London, SW7 2AZ, UK

Email: p.fromme@ucl.ac.uk

Running title: Guided Wave Scattering at Delaminations

7th April 2016

Abstract

Carbon fiber laminate composites are increasingly employed for aerospace structures as they offer advantages, such as a good strength to weight ratio. However, impact during the operation and servicing of the aircraft can lead to barely visible and difficult to detect damage. Depending on the severity of the impact, fiber and matrix breakage or delaminations can occur, reducing the load carrying capacity of the structure. Efficient nondestructive testing and structural health monitoring of composite panels can be achieved using guided ultrasonic waves propagating along the structure. The scattering of the A_0 Lamb wave mode at delaminations was investigated using a full three-dimensional (3D) Finite Element (FE) analysis. The influence of the delamination geometry (size and depth) was systematically evaluated. In addition to the depth dependency a significant influence of the delamination width due to sideways reflection of the guided waves within the delamination area was found. Mixed-mode defects were simulated using a combined model of delamination with localized material degradation. The guided wave scattering at cross-ply composite plates with impact damage was measured experimentally using a non-contact laser interferometer. Good agreement between experiments and FE predictions using the mixed-mode model for an approximation of the impact damage was found.

PACS numbers: 43.40.Fz, 43.35.Zc, 43.35.Cg, 43.40.Le

Keywords: Lamb Waves, Composites, Impact Damage, Finite Element (3D FEA)

I. INTRODUCTION

The usage of composite materials in aerospace structures has increased significantly as they offer significant advantages such as an excellent strength to weight capacity. However, the combination of carbon fibers and epoxy matrix in typical carbon-fiber reinforced polymer (CFRP) pre-preg composites is susceptible to impact loading. Low-velocity impact can induce barely visible damage[1], including matrix cracking, delamination, and fiber breakage, that can reduce the integrity of the structure[2]. Evidence of extensive delamination in the region adjacent to the impact zone has been shown[3] and it was found that this could reduce the overall load bearing capacity by up to 80%[4]. In contrast to matrix cracks or fiber breakage, delamination can occur in the absence of any visible surface damage, making it difficult to detect by visual inspection[5]. Therefore, it is important to efficiently monitor the composite structure during its service life to detect such damage and to ensure the safe operation of the structure. Guided ultrasonic waves (GUW) have the potential for the efficient nondestructive monitoring of large structures, as they can propagate over considerable distances at low excitation frequencies. This could significantly reduce the inspection time for large structures and be employed as part of a structural health monitoring (SHM) system[6, 7].

However, the scattering of guided waves by delaminations in a composite plate is a complex problem[8]. The propagation characteristics of the guided waves are complicated due to the anisotropic and inhomogeneous properties of the composites[9, 10]. Together with typically high attenuation values for CFRP, this makes monitoring and inspection using higher guided wave modes difficult and only limited work has been reported[11]. Typically it has been found to be advantageous to operate with a single wave mode at low frequency in order to avoid complications in the signal analysis and high attenuation[1]. The fundamental symmetric mode S_0 has attractive properties, as at low frequency it has limited dispersion and the fastest propagation velocity. However, the velocity depends strongly on the propagation direction relative to the composite layup fiber direction and the S_0 mode is typically coupled with the SH_0 mode[12]. Furthermore, it has been reported that the S_0 mode is not sensitive to delaminations between plies being under zero shear stress condition[13]. Recently significant effort has been focused on the fundamental anti-symmetric mode A_0, which has a shorter wavelength than the S_0 mode[14] and thus in principle better sensitivity for defect detection. Furthermore, the directionality of the wave propagation characteristics is significantly less dependent on the anisotropic material properties, leading to similar velocities in all directions for quasi-isotropic and cross-ply (0/90) layups[12].

The A_0 mode has been employed to detect different types of damage, such as cracking, fatigue and delaminations in composite structures[15]. It has been demonstrated that the A_0 mode tends to be more sensitive to delaminations than the S_0 mode and can detect delaminations at any depth[16]. Mode conversion from the A_0 to S_0 mode was observed when the guided wave interferes with the delamination boundaries[17], confirmed from experimental work[18]. Delaminations can in principle be located by estimating the propagation speed and time of flight from the reflected signal[19]. It was found that separate reflections from the delamination edges appear when the delamination length increases (relative to the wavelength)[20]. Work was performed on composites subjected to impact damage[21, 22]. From numerical simulations to characterize the scattering pattern generated at a circular delamination, it was found that the amplitudes around the delamination showed a large forward scattered wave relative to the reflected pulse[8].

Numerical models have been developed to characterize impact damage on composite plates, mostly employing 2D FE models of wave propagation and scattering in composites[13, 17, 23]. It was also observed that there is no converted S_0 mode when the A_0 mode encounters delaminations located at a symmetric interface. The combination of several damage mechanisms for realistic impact damage in laminated composites makes the accurate modelling more challenging, with limited studies employing full 3D analysis[24]. Recent work[25] has demonstrated that 3D simulations can accurately predict the scattering characteristics of guided waves at a circular-shaped delamination. The directivity pattern of the scattered A_0 wave mode around a defect representing cracking in the composite materials, modeled as a 3D conical shape with reduced material properties, has been predicted[26]. Impact damage was characterized using an X-ray computed tomography scan of a damaged composite sample and used as the basis for a numerical model implementing the complex 3D delamination geometry to investigate the interaction of guided waves with impact damage[27].

The focus of this contribution is the understanding of the interaction of the A_0 guided wave mode with delaminations, and a systematic study of the influence of the delamination size (length and width) and depth on the wave scattering was conducted using 3D FE simulations. Scattering of the A_0 guided wave mode at impact damage was observed experimentally, with increased amplitude at the impact location, and a repeatable scattering pattern with significant amplitude reduction of the guided wave propagating past the damage location[28]. Multi-mode impact damage was modelled as an additional reduction of material stiffness and the predicted wave scattering was compared to experimental results for impact damage.

II. EXPERIMENTAL GUIDED WAVE MEASUREMENT OF IMPACT DAMAGE

Two specimens were supplied by the Composite Systems Innovation Centre, University of Sheffield, which had been investigated in a separate study[29]. The composite plates (990 mm x 110 mm x 2 mm) were fabricated with unidirectional pre-pregs by autoclave cure using Cytec 977-2 / Tenax HTS cross-ply laminates (Fig. 1a). The plates consist of 8 pre-preg layers with a symmetric layup sequence of $[0/90]_{2s}$. Additionally, the plates contain a 25 µm thick polymide film and an 18 µm thick layer of flexible printed circuit boards for electrical resistance measurements[29]. The specimens had been subjected to a 7.4 J impact damage using a hemispherical 15 mm impactor head and following standard drop weight impact procedures. A small degree of fiber fracture and indentation was visible on the surface of the plates (Fig. 1b). For one of the plates a standard ultrasonic C-scan had shown an extensive delamination around the impact location[30]. A piezoelectric transducer to excite the A_0 guided wave mode, consisting of a piezoelectric disc (Ferroperm Pz27, 5 mm diameter, 2 mm thickness) and a brass backing mass (5 mm diameter, 6 mm height), was glued onto the plate with Loctite 2-part epoxy 100 mm from the center of the impact damage. The excitation signal was a 5 cycle sinusoidal tone burst modulated by a Hanning window with a center frequency of 100 kHz, generated in a programmable function generator and amplified to about 200 Vpp. The velocity of the out-of-plane displacement was measured using a laser vibrometer fixed to a scanning rig and moved parallel to the specimen. The time traces of the received signals were filtered using a band-pass filter (4th order Butterworth, cut-off frequencies 75 – 125 kHz) and were recorded and averaged (20 averages) using a digital storage oscilloscope. All signals were saved to a PC and further analyzed using Matlab. The maxima of the signal envelopes were obtained using Hilbert transform and evaluated. Two types of scans were performed; (i) horizontal line scans over a length of 200 mm from the transducer location in both directions with 1 mm step size; and (ii) circular scans with 30 mm radius measured every 5° around the excitation location, impact damage, and a symmetrically located undamaged area. Measurements on the undamaged part of the specimens were performed as a baseline measurement and to study the wave propagation characteristics of the A_0 Lamb wave mode in the undamaged composite plates for comparison to the FE simulations.

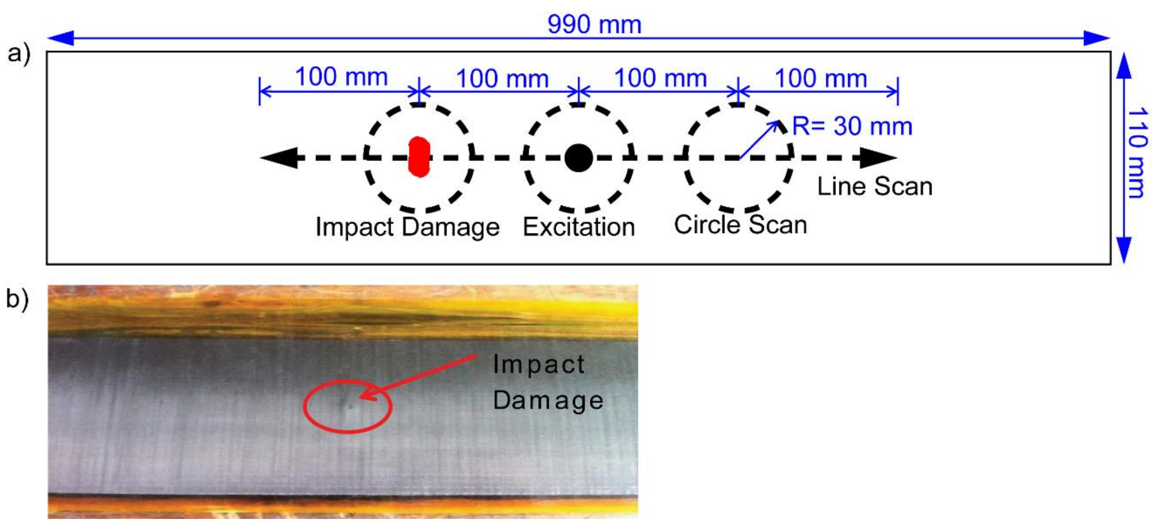

Figure 1: a) Schematic of cross-ply plates and measurement locations (not to scale); b) photo of specimen with barely visible impact damage (marked).

III. FINITE ELEMENT MODEL

The full 3D FE model of a large, layered composite plate with dimensions of 1000 mm x 1000 mm x 2 mm was defined using a program in MATLAB to specify the model and damage parameters. The description of the 8 individual layers with the same lay-up as the experimental specimens ($[0/90]_{2s}$) was implemented. The individual layers were modeled according to material properties of a unidirectional composite plate[10]. Rayleigh damping was set to ß = 30 ns to match the guided wave attenuation measured for the undamaged part of the composite specimens. Element size of 1 mm in the x- and y- directions (along the plate) and 0.25 mm in the z-direction (one element per layer through thickness) was employed, resulting in 8 million elements to model the plate. The element type was chosen as an 8-node linear brick element with reduced integration (C3D8R). The employed element size and time step fulfill the usual stability criteria of at least 10 elements per wavelength[31]. The wave propagation in the undamaged plate was verified against theoretical predictions and was found to be accurate (e.g., simulation phase velocity within 1% of theoretical value predicted using Disperse software[32]).

An additional layer of FE nodes along the delaminated area with the same co-ordinates, but not connected to the coinciding nodes, was created. Two separated layers of elements were thus defined, connected to the respective nodes along the delaminated area. This simulates two free surfaces which do not interact and represents a zero-volume delamination. Both rectangular and circular delamination shapes were modeled, approximating the circular shape with the Cartesian grid. The size (length and width) of the delamination was varied in the range of 10 mm to 50 mm, and the depth of delamination was changed in 0.25 mm steps.

Additionally a large delamination (200 mm x 200 mm) at 1 mm depth and an undamaged plate as the baseline case were modelled. For the investigation of multi-mode defects, the delamination was placed at 0.5 mm and 1 mm depth and a matching area of reduced stiffness properties (25%, 50%, and 75% reduction) through the thickness was modelled. Out-of-plane excitation was introduced as a point force to selectively generate an A_0 Lamb wave propagating along the plate[33, 34]. The excitation signal consisted of a 5 cycle sinusoidal tone burst modulated by a Hanning window, as for the experiments. The excitation location was placed 100 mm from the center of the delamination to match the experimental setup (200 mm for large delamination model). The out-of-plane displacement was monitored at the same locations as for the line and circular scans performed experimentally. For the circular scans the signal was interpolated between the 4 adjacent nodes around the monitoring location. Hilbert transform was used to extract the maximum of the signal envelopes for each monitoring node. Additionally the incident wave pulse was monitored on the matching nodes of the baseline simulation for the undamaged plate. The amplitude of the scattered wave was isolated by subtracting the time traces and recording the maximum amplitude of the envelope of the difference signal.

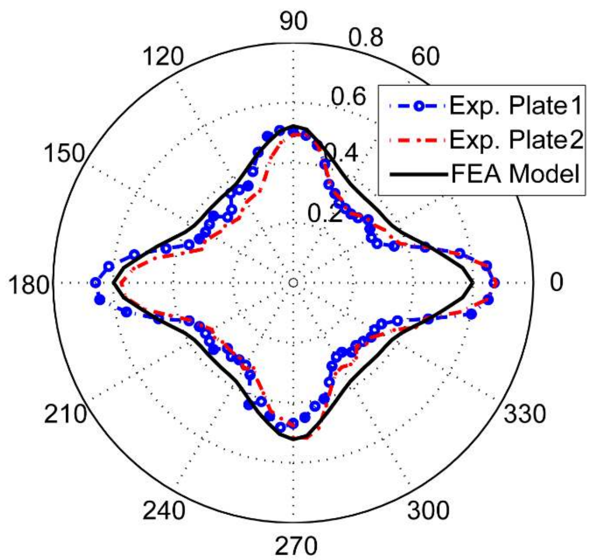

Figure 2 (color online): Comparison between experimental results for 2 plate specimens and FE simulations for amplitude circular scan (30 mm radius) around excitation location; 100 kHz center frequency.

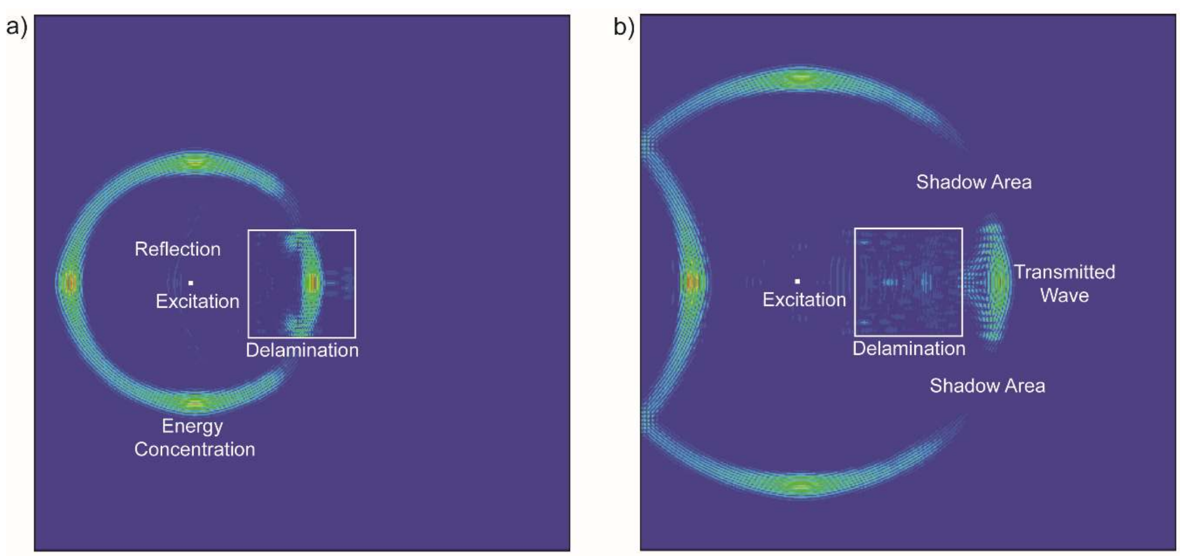

Figure 3 (color online): FE simulation of guided wave stress field (von Mises): a) 200 μs; b) 360 μs; 200 mm x 200 mm rectangular delamination (1 mm depth); 100 kHz center frequency.

IV. RESULTS AND DISCUSSION

A. Interaction with a large delamination

To validate the FE simulations, the amplitude of the excited A_0 mode pulse on a circle around the excitation location was compared between the measurements for the 2 composite specimens and the FE simulations. Figure 2 shows the expected amplitude pattern with higher amplitude along the 0° and 90° fiber directions. Good repeatability of the amplitude pattern for the two composite specimens and a good general agreement with the prediction from the FE simulation can be observed. Due to the symmetric lay-up of the cross-ply plate the top and bottom outer layers are both in the 0° direction and lead to slightly higher bending stiffness in this direction. This can be seen to result in slightly higher amplitude in the 0° direction compared to the 90° direction. The FE simulations predict slightly higher amplitude at 45° directions to the fiber orientation and slightly underestimates the amplitude increase in the 0° direction, but matches the experimental pattern overall well.

The interaction of an incident A_0 wave mode with a large square delamination (200 mm x 200 mm) positioned at the symmetrical plane (1 mm depth) of the 2 mm thick cross-ply composite plate was simulated. Figure 3a shows the snapshot at 200 μs as the incident A_0 mode has propagated into the delamination area. As expected, the amplitudes of the excited wave are higher in the 0° and 90° fibre directions and a small entry reflection from the delamination can be observed. Ahead of the main A_0 pulse on top of the delamination a mode converted S_0 pulse can be observed with higher propagation velocity. As the delamination is symmetric through the depth only the A_0 mode propagates in the undamaged plate. A sideways reflection of the A_0 mode at the upper and lower boundaries of the delamination can be observed due to the lower acoustic impedance of the delamination area (reduced thickness). This leads to a shadow area with lower amplitude next to the delamination. This can be observed more clearly from the second time snapshot at 360 μs in Fig. 3b. The transmitted A_0 pulse has high amplitude in the horizontal direction with a shadow area with lower amplitudes above and below. A significant trapping of the wave due to reflections inside the delamination area can also be observed. Experimental observations[35] confirmed such multiple reflections leading to high wave energy on top of the delamination, which could serve as a marker for localizing defects.

Figure 4a shows the time trace monitored between the excitation and delamination locations. A reflected wave pulse at 110 μs can be observed with about 10% of the amplitude of the incident wave pulse at 44 μs. In principle the time difference can be used to approximately localize the delamination entry[19]. However, combined with the attenuation and beam spread, the entry reflection has rather low amplitude, limiting the practical detection range in composites. Figure 4b shows the time trace recorded behind the delamination (forward scattering). The arrival time of the largest transmitted wave pulse at 270 μs corresponds to the main transmitted $A_0A_0A_0$ wave group (propagating as A_0 mode across the delamination). The arrival of the $A_0S_0A_0$ wave group (propagating as S_0 mode across the delamination) is observed earlier at 140 μs, due to the higher velocity of the S_0 mode across the large delamination[17]. Multiple reflected S_0 pulses can also be observed between the $A_0S_0A_0$ and $A_0A_0A_0$ pulses, with small amplitudes. This wave group keeps reflecting at the delamination boundaries and for the symmetrical delamination is confined to the delamination area. For large delaminations the faster transmitted wave pulse could serve as an indicator of a delamination, as the arrival time difference correlates to the delamination length.

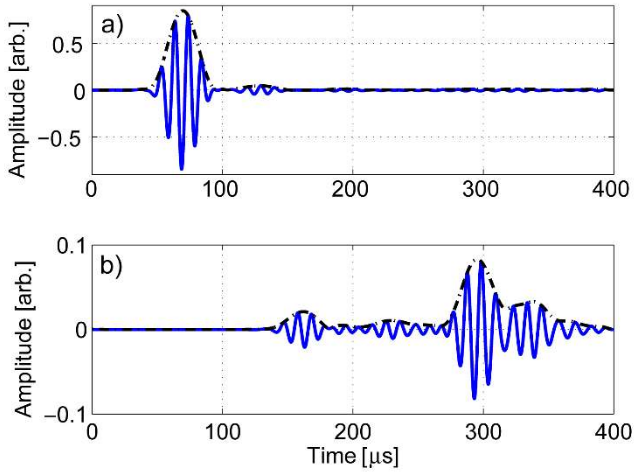

Figure 4 (color online): FE simulation of guided wave time signals for a 200 mm x 200 mm rectangular delamination (1 mm depth); a) 40 mm before delamination, b) 40 mm behind delamination; 100 kHz center frequency.

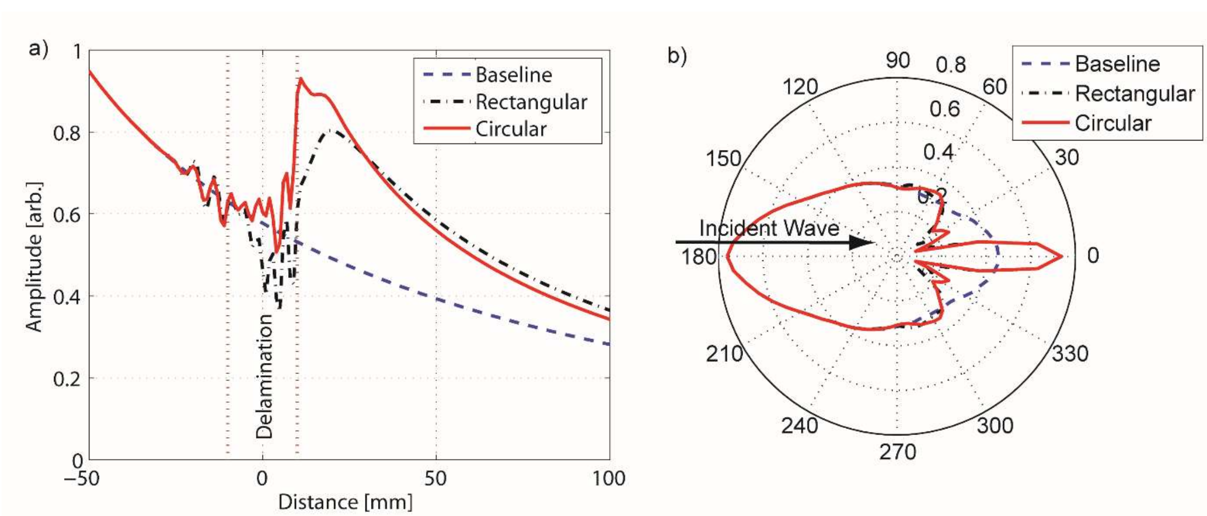

Figure 5 (color online): FE simulations for scattering at different delamination shape; baseline, rectangular delamination (20 mm x 20 mm); circular delamination (20 mm diameter); a) amplitude across defect area; b) amplitude circular scan; 100 kHz center frequency; 1 mm delamination depth.

B. Influence of delamination shape

In practice impact leads to irregularly shaped damage patterns, with delaminations often observed to have an approximately oval shape[3]. In this section it is considered whether a simple rectangular delamination shape can be used, which is straight-forward to implement in a FE model. Two regular shapes to represent a delamination are investigated: a rectangular-shaped delamination (dimensions: 20 mm x 20 mm) and a circular-shaped delamination (diameter: 20 mm). As can be seen from Fig. 5, both models resulted in comparable amplitude patterns, especially for the forward propagating wave. The peak amplitudes close to the circular shaped delamination (Fig. 5a) were seen to be slightly higher compared to the peaks from the square shaped delamination, and small differences in the angular scattering pattern were observed, particularly in the 30° and 330° directions (Fig. 5b), due to the different shapes causing slightly different scattering in these directions. It was observed that the circular and rectangular shaped delaminations of the same maximum extent (diameter matching rectangle) resulted in overall very similar scattering patterns and amplitudes. This confirms that the maximum length and width of the delamination are expected to have an influence on the guided wave scattering. Therefore, a simple and easy to implement rectangular shape was chosen for further FE modeling and analysis.

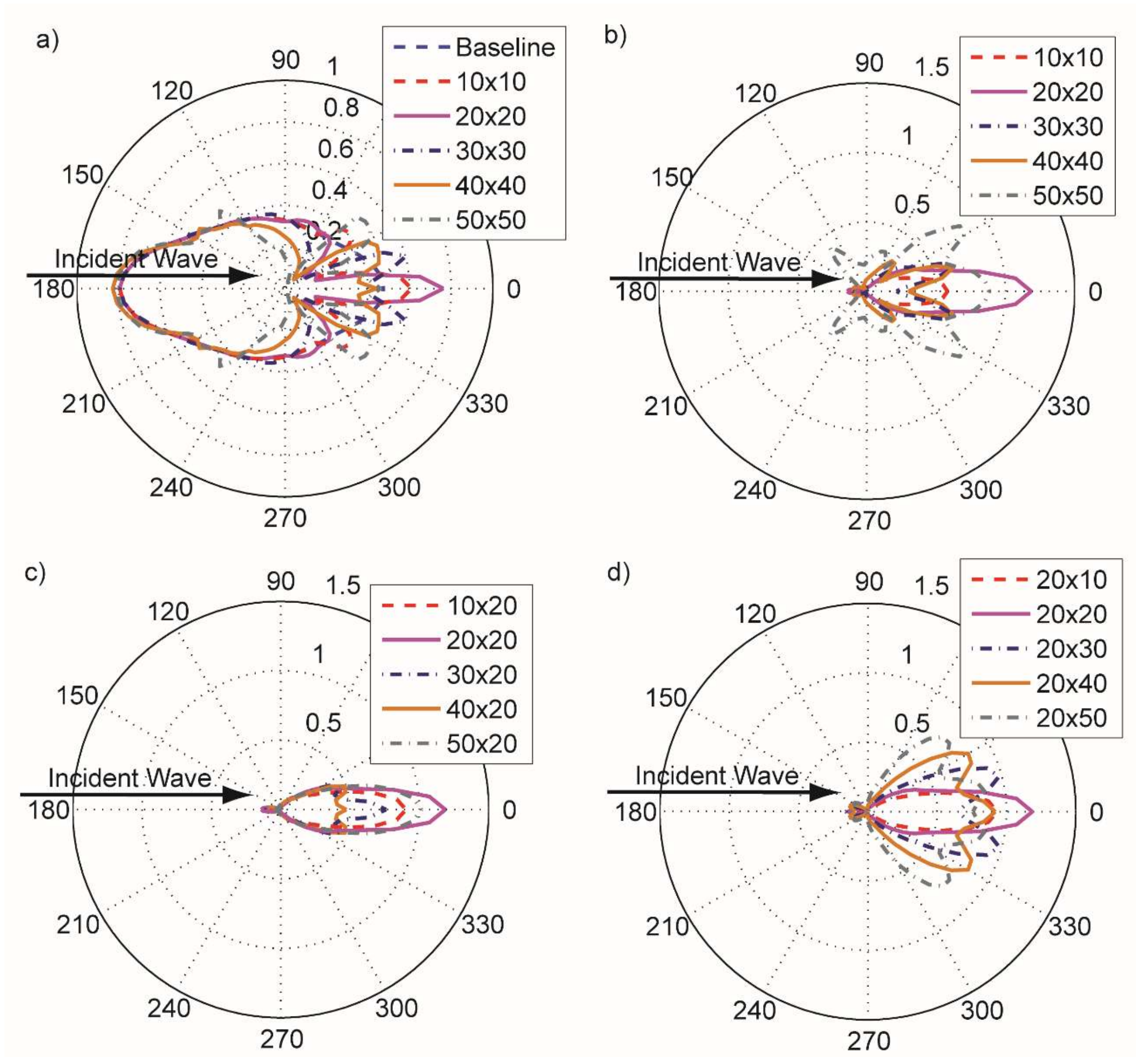

Figure 6 (color online): FE simulations for scattering at different delamination sizes (1 mm depth); a) amplitude circular scan (square delaminations); b) scattered difference amplitude circular scan (square delaminations); c) scattered difference amplitude circular scan (varied delamination length); d) scattered difference amplitude circular scan (varied delamination width); 100 kHz center frequency; delamination dimensions in mm.

C. Influence of delamination size

The angular amplitude pattern of the A_0 mode scattered at square delaminations with varying size at depth 1 mm can be seen in Fig. 6a. The backward scattered amplitudes (around 180°) show a regular pattern similar to the baseline data. Different forward scattering patterns can be observed at angles between 270° and 90°. For small delamination sizes (10 mm x 10 mm, 20 mm x 20 mm) comparable to the wavelength of the A_0 mode (15 mm) a large amplitude in the 0° direction and a reduced amplitude up to about +/-30° can be observed. For larger delamination sizes the forward scattering forms side lobes which, with increasing delamination size, move away from the main forward direction (0°), and a smaller forward amplitude is seen. Amplitude reduction for a wider range in the sideways direction up to about 90° for the largest considered delamination size (50 mm x 50 mm) was found. The amplitude of the scattered wave was isolated by subtracting the incident time traces from the baseline FE simulation and recording the maximum amplitude of the envelope of the difference signal (Fig. 6b). Forward scattering around the 0° direction was observed for the smallest considered delamination size (10 mm x 10 mm), increasing in magnitude for the 20 mm x 20 mm delamination. For this case the complex magnitude in the 0° direction is larger than the baseline amplitude as the forward scattered wave is out of phase with the baseline case (due to the change in propagation velocity across the thinner sub-lamina of the delamination). As the delamination size increases further, the scattered amplitude side lobes move away from the 0° direction, leading to the scattering pattern observed in Fig. 6a. In order to separate the influence of the delamination length and width, two sets of simulations were performed, varying these independently from 10 mm to 50 mm. As shown in Fig. 6c the angular scattering pattern for a symmetrically located delamination is almost independent of the delamination length with mostly only changes in the forward scattering amplitude (0°). No clear pattern of the magnitude of the forward scattering was found, as different delamination lengths lead to different phase changes compared to the propagation in the undamaged plate (baseline). Interestingly, there is a small back scattered amplitude (180° direction) for delamination lengths larger than 20 mm. This could be related to a reduced interference between reflections from the entrance and the exit of delaminations due to the increasing time delay, as has been observed in the case of a large delamination model[20]. Fig. 6d shows the influence of the delamination width on the angular scattering pattern. For delamination sizes larger than the wavelength of the A_0 mode, side lobes form and move away from the 0° direction with increasing delamination size. Based on the observations for the large delamination (Fig. 3), the directivity of the side lobes is related to the wave reflection at the sides of the delamination and energy trapping within the delamination. The geometry of the shadowed area at the delamination sides matches the angular directivity seen in Fig. 6d and can be approximated from geometric considerations (Fig. 3). This implies that the distance between the wave source (excitation) and the delamination has an influence on the observed scattering pattern, especially for the defect located close to the source, and should be taken into consideration for SHM applications[34]. The delamination width therefore has an important influence on the angular scattering pattern, as well as on the forward scattered amplitude, which cannot be captured using 2D FE simulations and should be considered using 3D FE simulations.

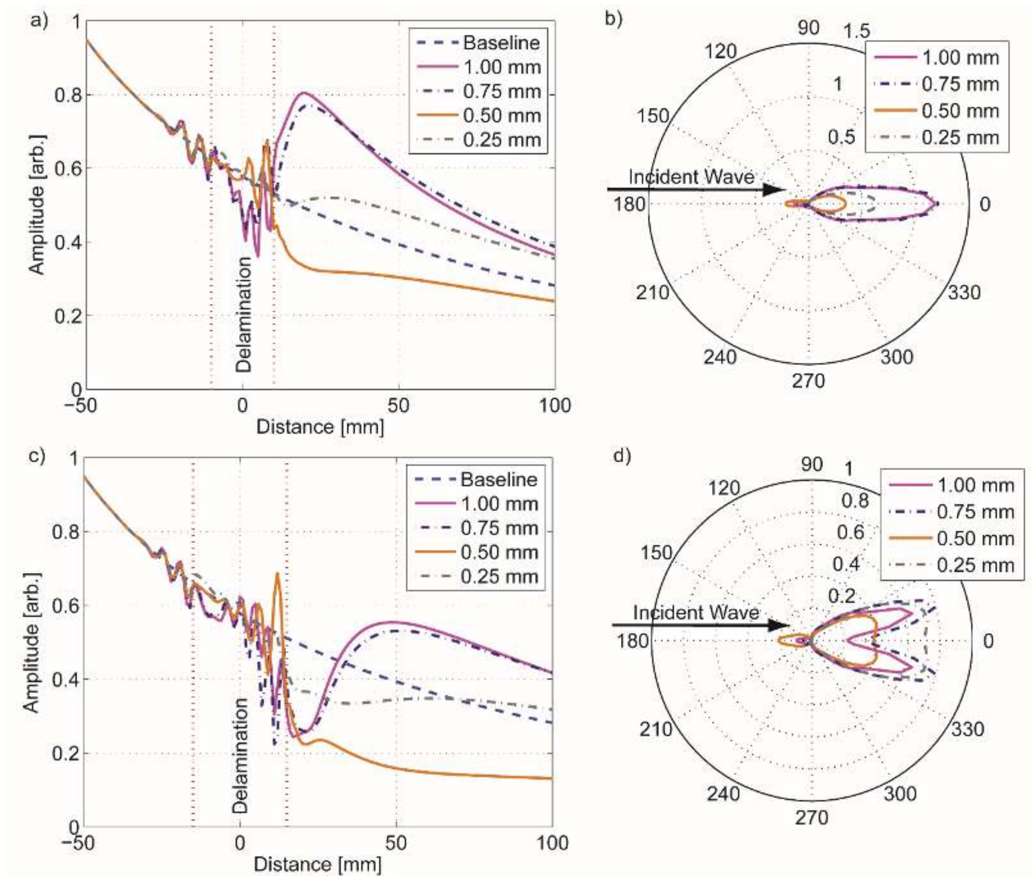

Figure 7 (color online): FE simulations for scattering at different delamination depth and size; a) amplitude across defect area (20 mm x 20 mm); b) scattered difference amplitude circular scan (20 mm x 20 mm); c) amplitude across defect area (30 mm x 30 mm); d) scattered difference amplitude circular scan (30 mm x 30 mm); 100 kHz center frequency.

D. Influence of delamination depth

The influence of the delamination depth on the mode conversion and forward scattering has been previously investigated from 2D FE simulations[13, 17, 33]. The scattered waves around square 20 mm x 20 mm and 30 mm x 30 mm delaminations placed at different depths were investigated. For both delamination sizes amplitude variations in the line scans can be seen in front and on top of the delamination due to the interference of the incident and reflected waves with only a small influence of the delamination depth (Fig. 7a/c). The effect of the delamination depth can be observed at the amplitude patterns behind the delamination region. The amplitudes of transmitted guided wave pulses past the delaminations located towards the center of the plate (0.75 mm and 1 mm depth) show a similar behaviour with an increase in amplitude due to the sideways reflection and energy trapping (Fig. 3). In contrast, for all case studies of different delamination sizes located at 0.50 mm depth an amplitude drop behind the delamination region was observed. When the delamination was located close to the plate surface (0.25 mm depth), the amplitude pattern can be seen to be close to the baseline data with limited change of the transmitted amplitudes. Using the baseline subtraction method, Fig. 7b/d shows the angular pattern of the isolated wave scattering. The scattering around delaminations at 0.75 mm and 1 mm depth close to the middle of the plate show similar behaviour with forward (20 mm x 20 mm) or side (30 mm x 30 mm) lobes of high amplitude (as observed in Fig. 6). The similar height of the sub-lamina on top and below the delamination for these cases leads to similar propagation velocities and acoustic impedances, and thus similar scattering patterns. For the case of the delamination placed close to the surface, i.e., 0.25 mm depth, Fig. 7b/d shows different magnitudes for the two delamination sizes as these lead to different phase shifts across the delamination. However, the change in amplitude of the transmitted waves for this depth was small (Fig. 7a/c). A different forward scattering pattern can be observed when the delamination is located at 0.50 mm depth with a consistent forward scattered wave leading to an amplitude drop in the line scans behind the delamination (Fig. 7a/c). The significant difference between wave speeds in the upper and lower sub-plates due to the unequal thicknesses of the sub-laminates contributes to the higher acoustic mismatch, leading to increased reflections and phase differences. This reduced forward scattered wave amplitude was observed as well for all other investigated delamination sizes at a depth of 0.5 mm, but not necessarily for other delamination depths. It thus has to be concluded that, for the regular delamination shape considered here, both either increased or decreased forward scattered amplitude of the A_0 wave mode can occur depending on the depth and size of the delamination and needs to be taken into consideration when devising damage detection algorithms for a SHM system.

E. Influence of reduction in material properties

As low-velocity impact has been shown to induce distributed microscopic fibre breaking and matrix cracking[3], and thus a local decay in the stiffness properties, a multi-mode defect consisting of a delamination with additional reduced stiffness properties was modelled[26]. Figure 8 shows a comparison of three FE models with a delamination and different material degradation compared to the model with only a delamination of 20 mm x 20 mm at 1 mm depth. It can be seen that there are increased amplitude peaks on the defective region for the three models with locally reduced stiffness. Since the wave velocity depends on the stiffness properties, a local change in the wave propagation velocity and thus an increased acoustic impedance mismatch occurs. This leads to an increase of the trapped energy and thus recorded wave amplitude with larger stiffness reductions. No significant influence of the stiffness property reduction on the angular scattering pattern was observed. In the region behind the defective area (Fig. 8), increasing stiffness reduction leads to a small drop in the forward scattered amplitude, but the overall influence on the guided wave scattering was found to be limited.

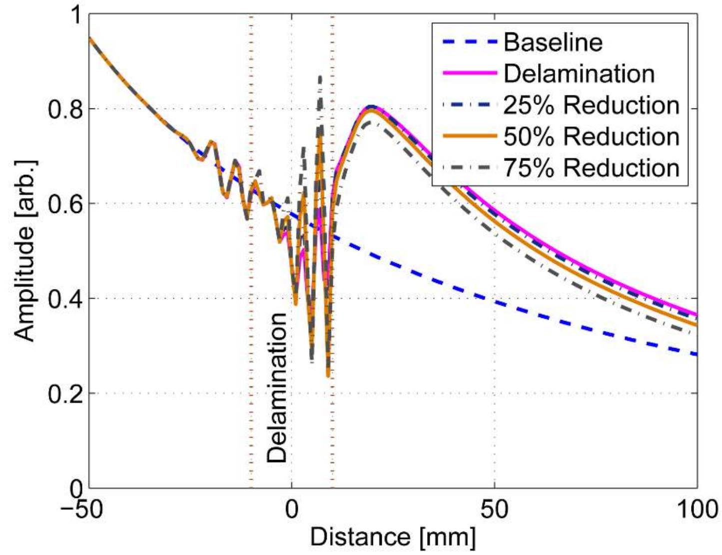

Figure 8 (color online): FE simulations for baseline, delamination (20 mm x 20 mm, 1 mm depth) and mixed-mode defect (delamination and 25%, 50%, 75% local material degradation); amplitude across defect area; 100 kHz center frequency.

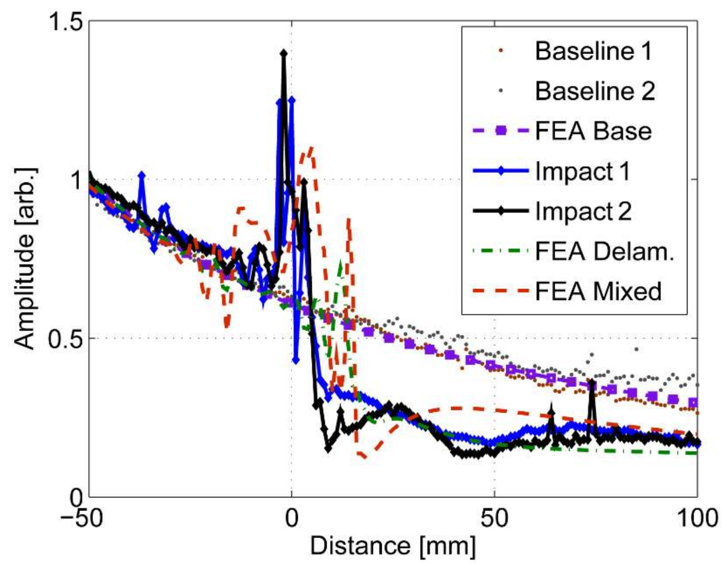

Figure 9 (color online): Comparison between experimental results (baseline and impact damage for 2 plates) and FE simulations for delamination (30 mm x 30 mm, 0.5 mm depth) and mixed-mode defect (delamination and 75% material degradation); amplitude across defect area; 100 kHz center frequency.

V. COMPARISON TO MEASURED SCATTERED FIELD AT IMPACT DAMAGE

Based on the observed scattering and the available information about the size and depth of the impact damage in the composite plates[28, 30], a comparison was made between the experimental measurements and FEA results for a delamination size of 30 mm x 30 mm located at 0.5 mm depth and a mixed-mode defect of the delamination with an additional, local 75% material degradation. The amplitudes measured along a line across the defects show high amplitudes in the damaged region and a significant amplitude drop behind the defective area compared to the baseline measurements on an undamaged part of the plate (Fig. 9). A reasonable match of the amplitude reduction with the FE simulation results for 0.5 mm delamination depth was found. As observed above, the FE model for a mixed-mode defect predicts higher amplitudes in the defective region, reasonably matching the experimental peaks for the two specimens. For the comparison of the angular pattern at the symmetrical, undamaged location (Fig. 10a), one can observe a reasonably good agreement between the baseline measurements and FE simulation. The amplitude in the incident wave direction (180°) is about twice the amplitude in the 0° direction, the same amplitude decrease observed from the line measurements. This matches the experimentally observed amplitude reduction along a line across the two undamaged plates, which was predicted accurately from the FE simulation (Fig. 9). The amplitudes are higher along the fiber directions due to the larger stiffness. For the damage case (Fig. 10b) the incident wave (180° direction) has a similar amplitude distribution as the baseline data (Fig. 10a) and no significant back-scattered amplitude is observed. Both FE simulations predict a decrease in the amplitudes behind the damage position (0°), with some smaller differences in the angular patterns (Fig. 10b).

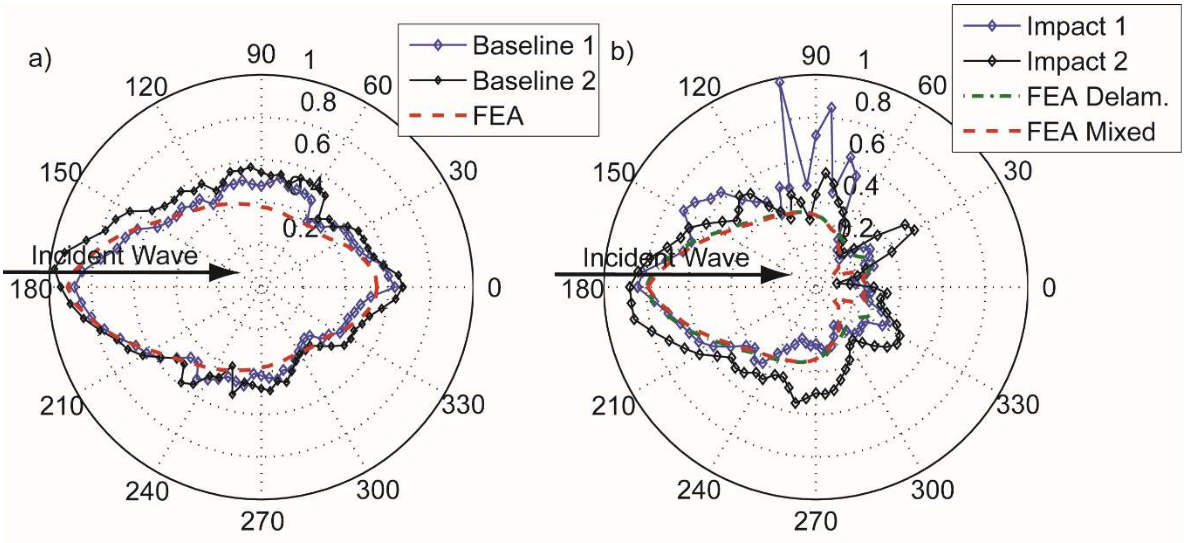

Figure 10 (color online): Comparison between experimental results (baseline and impact damage for 2 plates) and FE simulations for delamination (30 mm x 30 mm, 0.5 mm depth) and mixed-mode defect (delamination and 75% material degradation): a) undamaged plate; b) impact damage; amplitude circular scan; 100 kHz center frequency.

For the circular measurement around the damage location, it can be seen that both FE results provide a good prediction of the experimental observations with reduced forward scattered amplitude. The experimental results show a more complicated behavior due the complex impact damage and shape. Especially in the 90° direction the measured amplitudes for the impact damage in plate 1 are higher than for plate 2 and in the 270° direction, suggesting a non-symmetric impact damage. The FE simulations provide a regular pattern compared to the experimental results as the impact damage was modelled as a symmetric, rectangular delamination with additional decreased stiffness, rather than the actual irregular impact shape.

VI. CONCLUSIONS

Scattering of the A_0 Lamb wave mode from delaminations in composite plates was investigated using a 3D FE model. It was shown that the exact delamination shape has only a small influence on the observed overall scattering pattern. Using a simple damage implementation in the FE simulations, the effects of delamination size and depth were investigated. It was demonstrated that the delamination width has a strong influence on the scattering directivity. The angular scattering pattern indicates the obstruction of the wave propagation path due to the width of the damaged area and energy trapping within the delamination. It was found that the angular pattern of the scattered wave field is almost independent of the delamination length, while the delamination depth has a significant influence on the magnitude of the scattered waves. The comparison of the FE simulations for a mixed-mode damage model to measurements for impact damage in two composite plates showed good agreement. The results show the importance of further investigations of the three-dimensional scattering characteristics of guided waves at impact damage and delaminations to improve the detection capability of permanently installed SHM systems for composite structures.

ACKNOWLEDGMENTS

Bibi Intan Suraya Murat gratefully acknowledges funding by the Ministry of Science, Technology and Innovation (MOSTI), Malaysia and Universiti Teknologi MARA (UiTM), Malaysia. The authors would like to thank the Composite Systems Innovation Centre, University of Sheffield, UK for the provision of the composite plates.

REFERENCES

[1] C. H. Zhong, A. J. Croxford, and P. D. Wilcox, "Remote inspection system for impact damage in large composite structure," Proc. R. Soc. A **471**, 20140631 (2015).

[2] H. Y. Choi, H. T. Wu, and F. Chang, "A new approach toward understanding damage mechanisms and mechanics of laminated composites due to low-velocity impact: Part II--analysis," J. Compos. Mater. **25**, 1012–1038 (1991).

[3] M. O. W. Richardson and M. J. Wisheart, "Review of low-velocity impact properties of composite materials," Compos. Part A **27**, 1123–1131 (1996).

[4] A. N. Vorontsov, G. K. Murzakhanov, and V. N. Shchugorev, "Delamination failure of composite structures," Mech. Compos. Mater. **25**, 723–737 (1990).

[5] I. G. Scott and C. M. Scala, "A review of non-destructive testing of composite materials," NDT Int. **15**, 75–86 (1982).

[6] J. L. Rose, "Ultrasonic guided waves in structural health monitoring," Key Eng. Mater. **270–273**, 14–21 (2004).

[7] J. S. Hall and J. E Michaels, "Multipath ultrasonic guided wave imaging in complex structures," Struct. Health Monit. **14**, 345-358 (2015).

[8] C.-T. Ng and M. Veidt, "Scattering of the fundamental anti-symmetric Lamb wave at delaminations in composite laminates," J. Acoust. Soc. Am. **129**, 1288-1296 (2011).

[9] M. Castaings and B. Hosten, "Guided waves propagating in sandwich structures made of anisotropic, viscoelastic, composite materials," J. Acoust. Soc. Am. **113**, 2622-2634 (2003).

[10] M. J. S. Lowe, G. Neau, and M. Deschamps, "Properties of guided waves in composite plates, and implications for NDE," in Rev. Prog. QNDE **23**, eds. D. O. Thompson and D.

E. Chimenti, AIP Conf. Proc. **700**, 214–221 (2004).

[11] Z. Su, L. Ye, and Y. Lu, "Guided Lamb waves for identification of damage in composite structures: A review," J. Sound Vib. **295**, 753–780 (2006).

[12] S. K. Datta and A. H. Shah, Elastic waves in composite media and structures: with applications to ultrasonic nondestructive evaluation. CRC Press, Boca Raton (2009).

[13] N. Guo and P. Cawley, "The interaction of Lamb waves with delaminations in composite laminates," J. Acoust. Soc. Am. **94**, 2240-2246 (1993).

[14] S. Grondel, C. Paget, C. Delebarre, J. Assaad, and K. Levin, "Design of optimal configuration for generating A(0) Lamb mode in a composite plate using piezoceramic transducers," J. Acoust. Soc. Am. **112**, 84–90 (2002).

[15] M. Castaings, D. Singh, and P. Viot, "Sizing of impact damages in composite materials using ultrasonic guided waves," NDT&E Int. **46**, 22–31 (2012).

[16] P. Guy, Y. Jayet, and L. Goujon, "Guided wave interaction with complex delaminations. Application to damage detection in composite structures," Proc. SPIE **5047**, 25–33 (2003).

[17] C. Ramadas, K. Balasubramaniam, M. Joshi, and C. V Krishnamurthy, "Interaction of guided Lamb waves with an asymmetrically located delamination in a laminated composite plate," Smart Mater. Struct. **19**, 065009 (2010).

[18] R. Kazys, A. Demcenko, E. Zukauskas, and L. Mazeika, "Air-coupled ultrasonic investigation of multi-layered composite materials," Ultrasonics **44**, E819–E822 (2006).

[19] N. Toyama, J. Noda, and T. Okabe, "Quantitative damage detection in cross-ply laminates using Lamb wave method," Compos. Sci. Technol. **63**, 1473–1479 (2003).

[20] C. H. Wang and L. R. F. Rose, "Wave reflection and transmission in beams containing delamination and inhomogeneity," J. Sound Vib. **264**, 851–872 (2003).

[21] T. Kundu, S. Das, S. A. Martin, and K. V. Jata, “Locating point of impact in anisotropic fiber reinforced composite plates,” Ultrasonics **48**, 193–201 (2008).

[22] K. Diamanti, J. M. Hodgkinson, and C. Soutis, “Detection of low-velocity impact damage in composite plates using Lamb waves,” Struct. Health Monit. **3**, 33–41 (2004).

[23] C. B. Pol and S. Banerjee, “Modeling and analysis of propagating guided wave modes in a laminated composite plate subject to transient surface excitations,” Wave Motion **50**, 964–978 (2013).

[24] O. Mesnil, C. A. C. Leckey, and M. Ruzzene, “Instantaneous wavenumber estimation for damage quantification in layered plate structures,” Proc. SPIE **9064**, 90640D (2014).

[25] C. T. Ng, M. Veidt, L. R. F. Rose, and C. H. Wang, “Analytical and finite element prediction of Lamb wave scattering at delaminations in quasi-isotropic composite laminates,” J. Sound Vib. **331**, 4870–4883 (2012).

[26] D. Singh, R. El Guerjouma, and M. Bentahar, “Interaction of fundamental Lamb modes with a point impact damaged zone in composite plates,” Proc. Societe Francaise d’Acoustique, Acoustics 2012, 2423–2428 (2012).

[27] C. A. C. Leckey, M. D. Rogge, and F. Raymond Parker, “Guided waves in anisotropic and quasi-isotropic aerospace composites: three-dimensional simulation and experiment,” Ultrasonics **54**, 385–394 (2014).

[28] B. I. S. Murat and P. Fromme, “Detection of impact damage in composite panels using guided ultrasonic waves,” Proc. SPIE **8695**, 869506 (2013).

[29] T. J. Swait, F. R. Jones, and S. A. Hayes, “A practical structural health monitoring system for carbon fibre reinforced composite based on electrical resistance,” Compos. Sci. Technol. **72**, 1515-1523 (2012).

[30] M. Endrizzi, B.I.S. Murat, P. Fromme, and A. Olivo, "Edge-illumination X-ray dark-field imaging for visualising defects in composite structures," Compos. Struct. **134**, 895-899 (2015).

[31] J. Virieux, "P-SV wave propagation in heterogeneous media: Velocity-stress finite-difference method," Geophysics **51**, 889–901 (1986).

[32] B. Pavlakovic, M. Lowe, D. Alleyne, and P. Cawley, "DISPERSE: A general purpose program for creating dispersion curves," in Rev. Prog. QNDE **16**, eds. D. O. Thompson and D. Chimenti, Plenum, New York, 185–192 (1997).

[33] T. Hayashi and K. Kawashima, "Multiple reflections of Lamb waves at a delamination," Ultrasonics **40**, 193-197 (2002).

[34] J. S. Hall, P. Fromme, and J. E. Michaels, "Guided Wave Damage Characterization via Minimum Variance Imaging with a Distributed Array of Ultrasonic Sensors," J. Nondestruct. Eval. **33**, 299-308 (2014).

[35] H. Sohn, D. Dutta, J. Y. Yang, H. J. Park, M. DeSimio, S. Olson, and E. Swenson, "Delamination detection in composites through guided wave field image processing," Compos. Sci. Technol. **71**, 1250–1256 (2011).